Guest Emission Processes in Doped Organic Light-Emitting Diodes: Use of Phthalocyanine and Naphthalocyanine Near-IR Dopants

Ware H. Flora, Hank K. Hall, and Neal R. Armstrong*

Department of Chemistry, University of Arizona, Tucson, Arizona 85721

Received: June 6, 2002; In Final Form: September 18, 2002

A series of near-IR emitting organic light-emitting diodes (OLEDs) have been prepared using poly(vinylcarbazole) (PVK) as the hole transport polymer, aluminum quinolate (Alq_3) or a sulfonamide derivative ($Al(qs)_3$) as the host dye (H), and phthalocyanine (Pc) or naphthalocyanine (NPc) dopants as guest dyes (G). The separation of the emission spectrum of the guest dye from that of the host dye allows for independent assessment of their relative efficiencies and correlation of these efficiencies with their tendencies toward charge capture and recombination reminiscent of solution electrogenerated chemiluminescent reactions. Although the absorbance spectra of the guest dyes are significantly separated from the emission spectra of the host dyes, the high molar absorptivities of the Pc and NPc dopants lead to Förster radii and relative energy-transfer (ET) efficiencies comparable to values previously obtained for quinacridone or rubrene dopants, which have been used to create intense green or yellow emission in Alq_3-based OLEDs. We show that hole capture by the guest dye from oxidized PVK, $PVK^{+\bullet}/G \rightarrow PVK/G^{+\bullet}$, followed by cross-reactions, $Alq_3^{-\bullet}(Al(qs)_3^{-\bullet})/G^{+\bullet} \rightarrow Alq_3(Al(qs)_3)/G^*$, can be an important charge-trapping (CT), light-producing pathway at sufficiently high concentrations of the guest dye. Relative efficiencies of Pc* or NPc* emission in these single-layer devices increased exponentially with the electrochemically predicted excess free energy for the oxidation of G to form $G^{+\bullet}$ by $PVK^{+\bullet}$.

Introduction

Thin-film organic light-emitting diode (OLED) technologies have now matured to the point where a wide range of both single- and double-layer vacuum-deposited and polymeric devices can be obtained with high efficiencies and reasonable lifetimes.[1−15] Ideal single-layer devices require equal (and high) rates of electron and hole injection at the cathode and anode, respectively and high and equal rates of electron and hole transport, so that charge recombination occurs exclusively in the center of the 100−200 nm thin-film device.[1−3,16]

The most successful technologies to date, however, have been devices with two organic layers, in which differences in electron affinity (EA) and ionization potential (IP) of the two layers confine mobile charges near the center of the device. Of these two layer devices, those based on aluminum trisquinolate (Alq_3) as the electron transporting and emissive layer, and bisarylamines (e.g., 4,4′-bis(*m*-tolylphenylamino)biphenyl (TPD), poly(vinylcarbazole) (PVK), or related hole-transporting polymers) have been the most studied[4−10,13−15] with device geometries such as [ITO/TPD(PVK)/Alq_3/Al(Mg)]. TPD(PVK) hole-transport layers (HTL) are typically deposited on an indium−tin oxide anode (ITO), followed by deposition of the Alq_3 emissive and electron-transporting layer (ETL) and a low-work-function cathode, for example, Mg, Al, or an Al cathode with a thin layer of LiF or CsF interposed between the metal and organic layers. Two-layer polymer systems, such as poly(paraphenylene vinylene) (PPV) and its dicyano derivative, with comparable differences in EA/IP appear to provide similar confinement of emissive-state production.[1,2]

In both single-layer and two-layer Alq_3-based OLEDs, two options exist for formation of the metal quinolate luminescent state, Alq_3*: (i) holes (the cation radical state $TPD^{+\bullet}$ or $PVK^{+\bullet}$) are transported to the HTL/Alq_3 interface, followed by diffusion/migration of this hole state to the Alq_3 layer (formation of $Alq_3^{+\bullet}$), followed by a recombination reaction in the Alq_3 layer with the electron-rich (anion radical) form, $Alq_3^{-\bullet}$,

$$Alq_3^{+\bullet} + Alq_3^{-\bullet} \rightarrow Alq_3^* + Alq_3 \quad (1)$$

or (ii) the cation radical state of the hole-transporting molecules, $TPD^{+\bullet}$ (or $PVK^{+\bullet}$), reacts directly with $Alq_3^{-\bullet}$ according to

$$TPD^{+\bullet}(PVK^{+\bullet}) + Alq_3^{-\bullet} \rightarrow Alq_3^* + TPD(PVK) \quad (2)$$

Electrogenerated chemiluminescence (ECL) reactions in solution have recently been studied as models of cross-reactions such as those in eq 2, using Alq_3, a sulfonamide derivative of this metal quinolate, $Al(qs)_3$ (Figure 1), a solution-soluble quinacridone, *N*,*N*′-diisoamyl quinacridone (DIQA), and various substituted TPDs with a wide range of first oxidation potentials.[16−19] The yield of Alq_3*, or related luminescent states in DIQA, was shown to be exponentially related to the excess free energy in eq 2, as predicted from Marcus theory for electron transfer:[20,21]

$$k \propto \exp[-(\Delta G - \lambda_R)^2/(4\lambda_R k_B T)] \quad (3)$$

where k is the electron-transfer rate coefficient in eq 2, ΔG is the excess free energy in this reaction estimated from the differences in voltammetric peak potentials ($\Delta E°$) for the reduction of $Alq_3(Al(qs)_3)$ to $Alq_3^{-\bullet}(Al(qs)_3^{-\bullet})$ and the oxidation of TPD(PVK) to $TPD^{+\bullet}(PVK^{+\bullet})$, λ_R is the overall reorganization

* To whom correspondence should be addressed. E-mail: nra@u.arizona.edu.

10.1021/jp021368g CCC: $25.00
Published on Web 12/12/2002

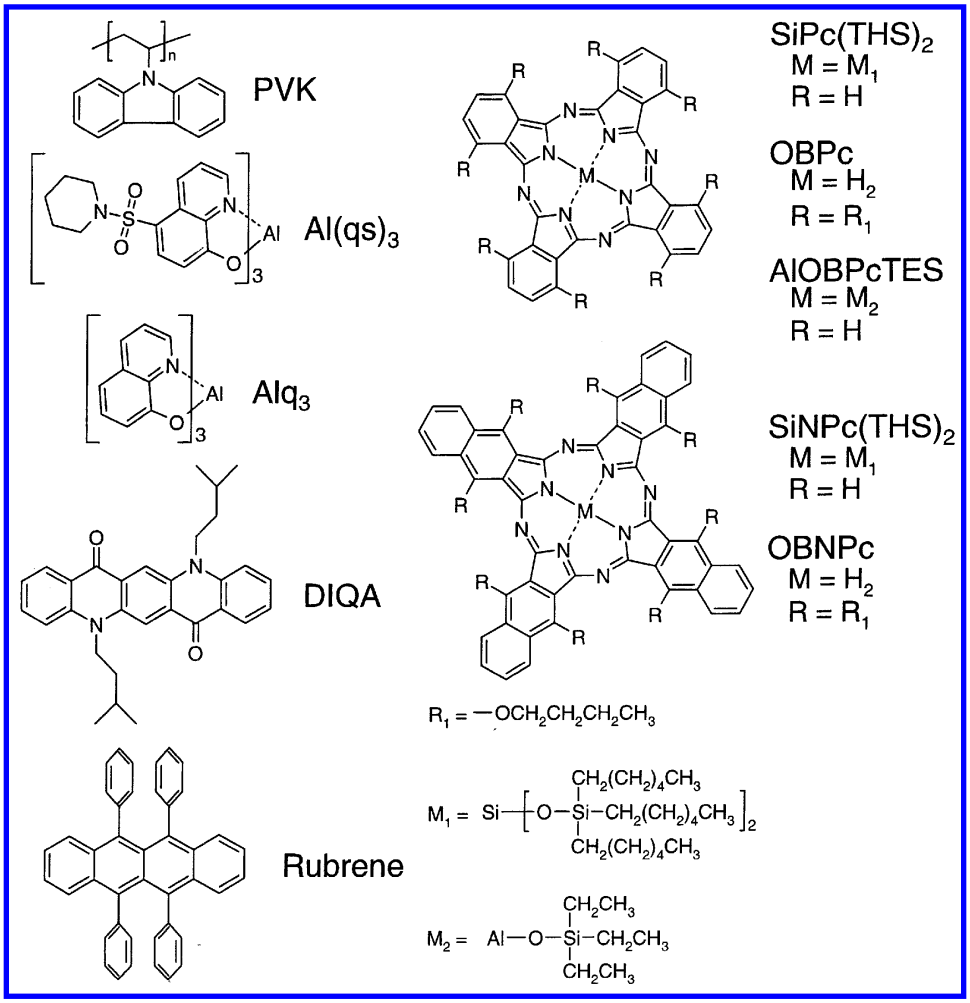

Figure 1. Structures for OLED materials: hole transport material (PVK), electron transport materials or hosts (Alq_3, $Al(qs)_3$), "typical" guests (DIQA, rubrene), solublized near-IR Pc guests ($SiPc(THS)_2$, OBPc, AlOBPcTES), and NPc guests ($SiNPc(THS)_2$, OBNPc).

energy needed to reach the activated state in these reactions, k_B is the Boltzmann constant, and T is the absolute temperature.

For purposes of mechanistic studies such as those presented here, it is convenient to create OLEDs using only one doped polymer layer, for example, Alq_3 doped into PVK at ca. 25% w/w, even though these devices typically do not produce electroluminescence efficiencies as high as two-layer vacuum-deposited devices. In single-layer Alq_3- or $Al(qs)_3$-doped PVK devices, only eq 2 is therefore likely to lead to formation of Alq_3* luminescent states.

OLED emission is often optimized by addition of small percentages of highly luminescent dopants designed to have good overlap of their absorbance spectra with the emission spectra of the host (maximizing the probability for Förster energy transfer).[5−7,22,23] Dexter energy transfer can generally be ignored at low guest dye concentrations because of the long-range nature of Förster energy transfer.[24] For Alq_3-based OLEDs, *N*,*N*′-bisalkyl-substituted quinacridones play this role of a highly luminescent, well-overlapped guest.[6,13,14] The highest efficiency OLEDs have been created with organometallic dopants, which harvest not only singlet states of the host dye but triplet states as well and have the lifetimes and phosphorescence efficiencies needed to ensure high overall device emission efficiencies.[9−11,24,25] Although these dopant dyes were designed to function primarily by Förster energy-transfer (ET) pathways,[26] it has recently become apparent that charge capture by these guest dyes, followed by recombination reactions leading to their emissive states, may be an important additional pathway.[25]

The quinacridone dye DIQA, added in small concentrations to Alq_3−PVK single-layer films (device geometry = [ITO/PVK + Alq_3 (14% w/w) + DIQA (0.1−10.0% w/w)/Mg]), completely quenches the Alq_3 photoluminescence (PL) response at low DIQA concentrations.[13,14] The Alq_3* electroluminescence (EL) response, however, is more efficiently quenched at all DIQA concentrations versus the PL response, suggesting that pathways other than energy transfer from Alq_3* to DIQA can contribute to guest emission in doped OLEDs.

Our recent ECL/voltammetric studies show that DIQA can act as an electron-acceptor toward $Alq_3^{-\bullet}$ (creating $DIQA^{-\bullet}$) and has the potential to act as an electron donor toward $PVK^{+\bullet}$ (creating $DIQA^{+\bullet}$).[16−19] Such charge-trapping (CT) reactions by this dopant have the potential to lead to luminescent state formation through the following cross-reactions:

$$PVK^{+\bullet} + DIQA^{-\bullet} \rightarrow DIQA^* + PVK \quad (4)$$

$$Alq_3^{-\bullet} + DIQA^{+\bullet} \rightarrow DIQA^* + Alq_3 \quad (5)$$

In both cases, the yield of the luminescent state, DIQA*, is expected to be exponentially related to the excess free energy in these reactions, as per eq 3.[16−19] The enhanced stability of both the radical cation and radical anion forms of these N,N′-alkylated quinacridones, relative to the radical forms of both

the hole-transport and electron-transport materials, makes it likely that doping with these kinds of molecules also increases the overall stability of these devices.[6,7,15,25,27]

Extending the emission of OLEDs into near-IR spectral regions is of interest[24,25] and provides for the use of a wider range of dopants for which the electrochemically generated radical anion and radical cation forms have been shown to be relatively stable. Previous ECL studies by Bard, Kenney, and co-workers showed that functionalized phthalocyanines and naphthalocyanines can provide near-IR emission by cross-reactions involving their radical states ($Pc^{+\bullet}/Pc^{-\bullet} \rightarrow Pc^* + Pc$).[28]

This paper summarizes both solution electrochemical studies and spectroscopic properties of various soluble phthalocyanine (Pc) and naphthalocyanine (NPc) guest (G) dyes (Figure 1), including Förster radii (R_0) for ET from the hosts (H) Alq_3 and $Al(qs)_3$. Although the peak absorbance of these guest dyes is significantly shifted from the peak luminescence of the hosts, their higher molar absorptivities result in ET probabilities that are comparable to those seen for both quinacridone and rubrene dopants. Because of the spectral separation between the host and the guest in these Pc and NPc systems, relative efficiencies of host and guest electroluminescence can be separately quantitated in the same device. For [ITO/(PVK + Alq_3($Al(qs)_3$) + G)/CsF/Al] device configurations, we show that hole capture by these guest dyes,

$$PVK^{+\bullet} + G \rightarrow PVK + G^{+\bullet} \quad (6)$$

followed by cross-reactions,

$$G^{+\bullet} + Alq_3{}^{-\bullet}(Al(qs)_3{}^{-\bullet}) \rightarrow G^* + Alq_3(Al(qs)_3) \quad (7)$$

is a viable charge-trapping (CT) pathway for creating G*. For the device types studied here, the probability for G* production initiated by CT is exponentially related to the excess free energy involved in the capture of a hole by the guest dye, as estimated from the solution electrochemical characterization of these materials.

Experimental Section

Voltammetric Characterization of Solution Redox Processes. The voltammetric characterization of the reduction and oxidation processes for Alq_3, $Al(qs)_3$, DIQA, and rubrene have previously been published.[16,17] Voltammograms for the other species were acquired with an EG&G Instruments 283 potentiostat, using a 500 μm diameter Pt working electrode, a freshly prepared Ag/AgCl pseudoreference electrode, and a Pt counter electrode, in N_2-degassed chloroform with 0.1 M tetrabutylammonium hexafluorophosphate (TBAHFP) supporting electrolyte. The working electrode was cleaned between each experiment by polishing with 0.3 μm alumina paste for 1 min, followed by copious solvent rinses. The reference electrode was prepared by plating a thin layer of AgCl onto a Ag wire from a saturated KCl solution. After each voltammetric experiment, ferrocene was added (ca. 1 mM), an additional voltammogram was recorded, and the potential axis was calibrated against the formal potential for the ferrocenium/ferrocene (Fc^+/Fc) redox couple.[29]

Luminescence/Absorbance Spectroscopy. A fiber-optic/charge-coupled-device-array spectrophotometer (Instruments S. A., Inc., Triax model) was used to measure device EL spectra. The spectrophotometer was corrected for variations in efficiency with emission wavelength by measuring dyes with known emission spectra.[30] A 10^{-3} M solution of quinine sulfate in 0.1 N H_2SO_4 was used for correction from 375 to 600 nm. The solution was placed in a cuvette holder that was modified to allow coupling of the optical fiber. Excitation was achieved with the 365 nm line of a UV lamp (UVP, model UVLS-24). A 10^{-5} M solution of 4-(dimethylamino)-4′-nitrostilbene (DMANS) in 1,2-dichlorobenzene was used for correction from 600 to 950 nm. Excitation was achieved with the 458 nm line of an Ar^+ laser (Ion Laser Technology, model 5500 ASL).

Molar absorptivity values and spectra were acquired by preparing known dilute solutions of the guest dyes in $CHCl_3$ and subsequent analysis with a CCD array spectrophotometer (Spectral Instruments, model 400). Solution fluorescence measurements were made on a Fluorolog-3 (Instruments, S. A., Inc.) with a xenon lamp source and a red-sensitive PMT (photomultiplier tube, 850 nm). To measure corrected emission spectra, the fluorimeter was corrected for variations in efficiency with emission wavelength using the calibration curve provided by the manufacturer.

To measure fluorescence quantum yields, corrected emission spectra were collected for all dyes immediately following an absorbance measurement of the same solution. Reference spectra for molecules with known quantum yields[30] were also acquired at the same excitation conditions. A solution of fluorescein in 0.1 M NaOH was used as reference for Alq_3, $Al(qs)_3$, DIQA, and rubrene, and a solution of cresyl violet perchlorate in methanol was used as reference for the Pc and NPc guests. The emission spectrum for OBNPc is past the cutoff of the fluorimeter PMT, so its spectrum was collected with the fiber-optic spectrophotometer, using a Hg−Xe arc lamp (Spectral Energy, model LPS251SR) with a 750 nm bandpass filter as the excitation source. Because a significant portion of OBNPc emission extends beyond the spectrophotometer correction region (950 nm), quantum yields could only be estimated in this configuration. The estimated value for quantum yield was obtained by extrapolating the correction curve using cresyl violet as a reference dye.

Device Fabrication/Characterization. ITO (optical science quality, Colorado Concept Coatings, LLC.) with a sheet resistance of 24 Ω/□ was cut into 1 in.^{2} substrates and cleaned by scrubbing with Triton X (Aldrich) detergent in deionized water (18 MΩ). The substrates were then sonicated in a Triton X solution for 20 min, rinsed with deionized water, sonicated in deionized water for 20 min, rinsed with ethanol, and sonicated in ethanol for 20 min. Substrates were transferred to an ulpa-filtered laminar-flow hood, where they were removed from the ethanol bath and dried in a stream of nitrogen. They were then masked and mounted for SiO deposition and transferred to the vacuum deposition chamber in a sealed container. A total of 200 nm of insulating SiO was next deposited through a mask on these cleaned ITO substrates at a rate of 0.3 nm/s from an alumina crucible (R. D. Mathis) at a chamber pressure of 1×10^{-5} Torr. This thin film was used to prevent electrical contact between the finally deposited Al cathode and the underlying ITO anode. The patterned substrates were then transferred back to the laminar-flow hood, where they were air-plasma-etched (Harrick, model PDC-32G) at 60 W for 15 min.

Spin-cast solutions containing PVK (14.2 mg/mL), Alq_3 or $Al(qs)_3$ (7.62×10^{-3} M effective concentration, 25% or 46% w/w, respectively), and a guest dye (up to 8 mol % of the host) were prepared. The substrates were removed from the plasma cleaner and immediately spin-coated (Integrated Technologies, Inc., model P6204) at 3000 rpm for 60 seconds. Devices were then masked and transferred to the cathode vacuum-deposition chamber.

In the cathode deposition chamber, 0.3 nm of CsF was deposited from an alumina crucible (R. D. Mathis) at a rate of

0.01 nm/s, followed by deposition of 150 nm of aluminum from an alumina-coated boat (R. D. Mathis) at a chamber pressure of 5×10^{-6} Torr. The cathode deposition pattern yields four distinct devices per substrate. The chamber was vented with nitrogen gas, and devices were transferred to a nitrogen-atmosphere glovebox (Vacuum Atmospheres Company) that is coupled to the cathode chamber, that is, following cathode deposition, the OLEDs were not exposed again to atmosphere.

Device substrates were seated into a custom-built clamp, which facilitates electrical contact to the cathodic contacts of the four devices and the ITO anode. In addition, this clamp facilitates the coupling of photodiode detectors (Hamamatsu) or a fiber-optic cable to couple the emission out of the glovebox to the CCD-array spectrometer discussed above. The photodiode current is passed through a current-to-voltage amplifier (Newport, model 1815-C), and a Kiethly 2400 SourceMeter is used to control bias voltage and measure device current. The entire measurement package was computer-interfaced to a LabView program (National Instruments) that controls the SourceMeter and measures device current and intensity.

All devices were conditioned by ramping the bias voltage from 0 to 25 V at a rate of 2 V/s, two times each, prior to measuring the EL spectrum at a bias of 25 V. The spectrophotometer entrance slit was set to 0.2 mm with a 10 s integration time.

The concentration of guest molecules in the PVK film (C_G) was calculated using the following expression:

$$C_G = d_{PVK}\left(\frac{m_G}{m_{PVK}}\right)\left(\frac{1}{MW_G}\right) \quad (8)$$

where d_{PVK} is the density of PVK (1.200 g/mL), m_G is the mass of the guest in the cast solution, m_{PVK} is the mass of PVK in the cast solution, and MW_G is the molecular weight of the guest. This calculation assumes that the density of the film is not influenced by the presence of the host and guest and that the mass ratio of guest to PVK is the same in the film as that in the cast solution. This relationship has been confirmed by redissolving the film and quantitating the amount of PVK and guest by absorbance methods. For the 1.6 mol % devices used to compare across guest molecules, this gives a C_G of 0.010 M. Using a similar expression for the host, we determined the concentration of the host in the film (C_H) to be 0.65 M.

Chemicals. Silicon(IV) phthalocyanine bis(trihexylsilyloxide) ($SiPc(THS)_2$, Aldrich), silicon 2,3-naphthalocyanine bis(trihexylsilyloxide) ($SiNPc(THS)_2$, Aldrich), aluminum 1,4,8,11,15,18,22,25-octabutoxy-29*H*,31*H*-phthalocyanine triethylsiloxide (AlOBPcTES, Aldrich), 1,4,8,11,15,18,22,25-octabutoxy-29*H*,31*H*-phthalocyanine (OBPc, Aldrich), 5,9,14,18,23,27,32,36-octabutoxy-2,3-naphthalocyanine (OBNPc, Aldrich), silicon(II) oxide (SiO_2, 99.99%, Alfa Aesar), aluminum wire (2.0 mm diam, 99.999%, Alfa Aesar), tetrabutylammonium hexafluorophosphate (TBAHFP, 98%, Aldrich), fluorescein, disodium salt (Eastman), cresyl violet perchlorate (Aldrich), 4-(dimethylamino)-4′-nitrostilbene (DMANS, 99.8%, Fluka), quinine sulfate dihydrate (99.0%, Fluka), H_2SO_4 (51%, Mallinckrodt), and 1,2-dichlorobenzene (99%, Aldrich) were used as received. $CHCl_3$ (98%, EM Science) was purified by distillation. Poly(9-vinylcarbazole) (PVK, $M_w \approx 10^6$, Aldrich) and ferrocene (Aldrich) were recrystallized from absolute ethanol. 8-Hydroxyquinoline, aluminum salt (Alq_3, 98%, Aldrich), and rubrene (Aldrich) were purified by vacuum sublimation. The synthesis of 8-hydroxy-5-piperdinylquinolinesulfonamide ($Al(qs)_3$) has been described previously.[31] The preparation of *N*,*N*′-diisoamyl quinacridone (DIQA) has also been published elsewhere.[14]

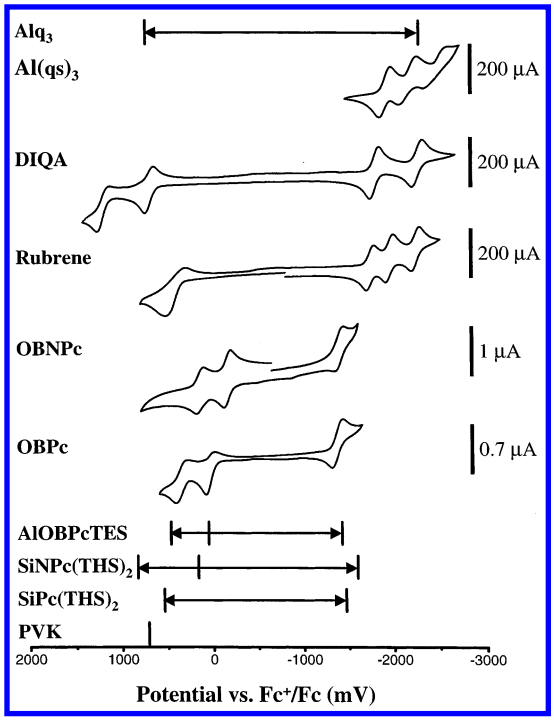

Figure 2. Cyclic voltammograms (CVs) for OLED materials referenced to the Fc^+/Fc redox couple. Some voltammograms are abbreviated with tick marks at the half-wave potential for the given process. Alq_3, $Al(qs)_3$, DIQA, and rubrene were acquired in 50:50 benzene/acetonitrile and are ranked by first reduction potential. Pc, NPc, and PVK CVs were acquired in $CHCl_3$ and are ranked by first oxidation potential. Reaction energies in Table 2 were estimated from differences in peak potentials for these different redox couples.

Results and Discussion

Solution Electrochemistry. Cyclic voltammograms for the species under study are presented in Figure 2, and first oxidation potentials ($E^{\circ\prime}_{Ox}$) and first reduction potentials ($E^{\circ\prime}_{Red}$) are summarized in Table 1. The potential axis is referenced to the Fc^+/Fc redox couple ($E^\circ = 0.46$ V vs SCE; 0.70 V vs NHE). To simplify the presentation, the E° values for some redox couples, estimated from the peak potentials in their voltammograms, are shown as tick marks. The $E^{\circ\prime}_{Ox}$ for the carbazole moieties in PVK was determined to be 0.71 V by voltammetrically characterizing both PVK thin films and solutions saturated with vinyl carbazole oligomers.

The first reduction process for Alq_3 is chemically reversible on the microsecond time scale, while the first reduction process for $Al(qs)_3$ occurs at ca. 0.3 V more positive and is chemically reversible on at least the 1−2 s time scale.[18] The first oxidation process for both quinolates is not chemically reversible on any time scale explored, which has a significant impact on device stability and the role of dopants in these technologies.[15,27]

The voltammograms for $SiPc(THS)_2$ and $SiNPc(THS)_2$ are consistent with previously reported voltammetric studies of silicon phthalocyanines and naphthalocyanines in which the central silicon is "end-capped" with solubilizing substituents.[28,32] It was shown by Bard and co-workers that for such dye solutions the working electrode could be cycled quickly between potentials for the first reduction and first oxidation of these species and that cation radical/anion radical recombination reactions, $Pc^{+\bullet}/Pc^{-\bullet}$ or $NPc^{+\bullet}/NPc^{-\bullet}$, in the adjacent diffusion layer led to formation of Pc* or NPc* states with subsequent emission

TABLE 1: Physical Constants for Host and Guest Dyes[a]

dye	$E^{\circ\prime}_{\mathrm{Red}}$ (V) vs Fc^+/Fc	$E^{\circ\prime}_{\mathrm{Ox}}$ (V) vs Fc^+/Fc	$\lambda_{\mathrm{max,abs}}$ (nm)	$\epsilon_{\lambda_{\mathrm{max}}}$ (M^{-1} cm^{-1})	$\lambda_{\mathrm{max,PL}}$ (nm)	Q	$\lambda_{\mathrm{max,EL}}$ (nm)[b]	$R_{0,\mathrm{Alq_3}}$ (Å)[c]	$R_{0,\mathrm{Al(qs)_3}}$ (Å)[c]
Alq_3	−2.30	0.71	387	7.0×10^3	525	0.29	517		
$Al(qs)_3$	−1.98	1.04	380	1.6×10^4	487	0.35	510		
DIQA	−1.81	0.68	523	3.1×10^4	538	1.00	525	31.4	37.1
rubrene	−1.75	0.43	529	5.5×10^3	559	0.54	553	29.9	35.3
$SiNPc(THS)_2$	−1.60	0.16	773	4.9×10^5	775	0.59	789	29.8	24.7
$SiPc(THS)_2$	−1.47	0.54	669	3.8×10^5	671	0.45	677	34.7	28.0
AlOBPcTES	−1.44	0.05	772	1.9×10^5	788	0.19	796	28.9	23.8
OBPc	−1.43	0.02	775	1.4×10^5	789	0.13	795	30.1	24.6
OBNPc	−1.40	−0.17	869	2.3×10^5	882	0.17[d]	879	24.0	18.8

[a] $CHCl_3$ is the solvent for all solution measurements. [b] Host dye values are for host-only devices. Guest dye values are for Alq_3−1.6 mol % guest devices. [c] Calculated using the refractive index of PVK. [d] An estimated value, based on an extrapolated correction curve.

at wavelengths close to those summarized below in our thin film OLEDs.[28] In general, the first and second oxidation and reduction processes for all dyes explored here were chemically reversible (e.g., OBNPc), although for some of these dyes (e.g., OBPc) there were slow chemical reactions (half-life of ca. 0.5 s) occurring to the first oxidation and reduction products, which made the voltammograms appear only partially reversible. On shorter time scales, relevant to the formation and recombination of charges in an OLED, the first oxidation and reduction processes for all dyes explored here produce stable products and symmetric voltammograms.

This electrochemical data indicates that DIQA, rubrene, and all of the Pc and NPc dyes are electron acceptors versus either $Alq_3^{-\bullet}$ or $Al(qs)_3^{-\bullet}$ ($H^{-\bullet} + G \rightarrow H + G^{-\bullet}$) with excess free energies in such electron-transfer processes varying from 0.17 to 0.90 eV. The data in Figure 2 also suggest that each of these dyes can act as electron donors to the oxidized form of PVK ($PVK^{+\bullet} + G \rightarrow PVK + G^{+\bullet}$) with excess free energies ranging from 0.03 to 0.88 eV for such processes. In devices in which Alq_3 or $Al(qs)_3$ and the guest dyes are surrounded by excess carbazole moieties from the PVK matrix, it can be expected that hole capture by the guest dye will be a significant first step in the creation of emitting Pc* or NPc* states.

Solution Spectroscopy. Normalized absorbance (solid lines) and normalized, corrected fluorescence spectra (dashed lines) are shown for all OLED guest dyes in $CHCl_3$ in Figure 3, along with the fluorescence spectra for the host dyes in $CHCl_3$. The wavelength of maximum absorbance ($\lambda_{\mathrm{max,abs}}$), molar absorptivity at maximum absorbance ($\epsilon_{\lambda_{\mathrm{max}}}$), and wavelength of maximum fluorescence intensity ($\lambda_{\mathrm{max,PL}}$) are listed in Table 1 for all dyes in $CHCl_3$. Comparable spectra were obtained for these dyes dissolved in the PVK matrix at concentrations present in the device. Spectroscopic data for Alq_3 and $Al(qs)_3$ are consistent with what has previously been reported,[31] as well as data for $SiPc(THS)_2$ and $SiNPc(THS)_2$.[28] Although these Pc and NPc molecules have triplet quantum yields of ca. 0.2,[33,34] phosphorescence measurements are neglected here, as well as in the EL spectra, because the singlet-to-triplet ratio should be constant for a given guest molecule at a fixed concentration in the device.[16] One would expect the same trends in relative guest emission efficiency to be observed in such measurements as those described here.

Solution fluorescence quantum yields for each host and guest dye (Q) were calculated according to

$$Q = Q_{\mathrm{R}}\left(\frac{A_{\mathrm{R}}}{A}\right)\left(\frac{I}{I_{\mathrm{R}}}\right)\left(\frac{n}{n_{\mathrm{R}}}\right)^2 \qquad (9)$$

where Q_{R} is the quantum yield of a reference dye (0.95 for fluorescein, 0.54 for cresyl violet),[30] A is the absorbance of a dilute solution of one of our guest or host dyes at the excitation wavelength, A_{R} is the absorbance of the reference dye solution, I is the corrected, integrated luminescence intensity of the analyte, I_{R} is the corrected, integrated luminescence intensity of the reference dye, n is the refractive index of the analyte solvent, and n_{R} is the refractive index of the reference dye solvent.[30] Values of Q are listed in Table 1. A value of $Q = 0.29$ for Alq_3 is comparable to that found in the solid state (0.30, 0.25).[23,35] It is likely that quantum yields for these dyes in the PVK film will differ slightly from solution values; however, we anticipate that their relative quantum efficiencies will not be altered versus solution measurements.

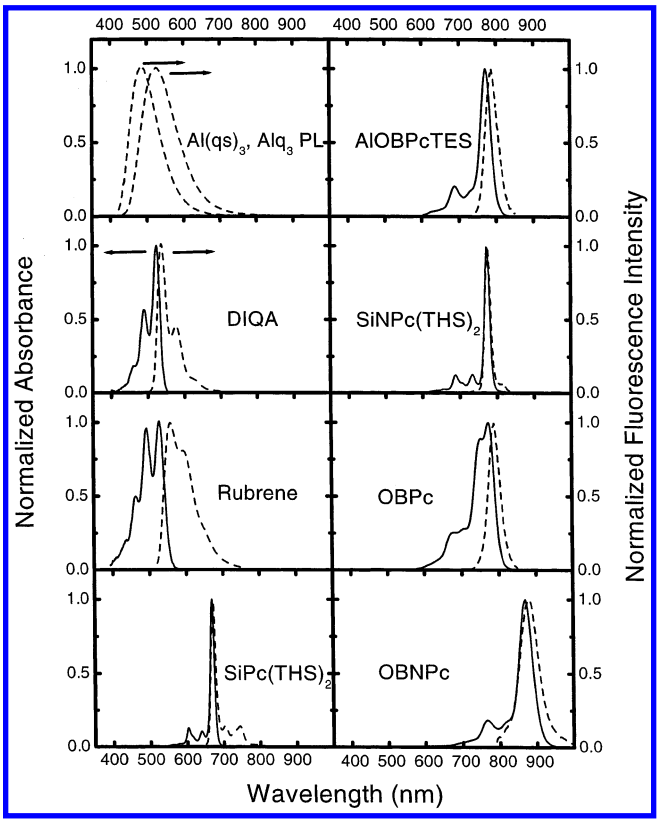

Figure 3. Normalized solution absorbance (solid lines) and corrected fluorescence (PL) spectra (dashed lines) of the host and guest dyes in $CHCl_3$. Absorbance spectra are normalized to a maximum absorbance of 1, and PL spectra are normalized to a maximum intensity of 1. The PL spectra for the hosts are presented in the first panel. The other panels contain the absorbance and PL spectra for each guest, ranked in order of increasing $\lambda_{\mathrm{max,abs}}$.

EL Spectra. All OLEDs showed current/voltage behavior typical of forward-biased diodes, with turn-on voltages of ca. 14 V and maximum luminance of ca. 200 cd/m^2 for Alq_3/PVK devices without guest dyes, typical of previous PVK-based

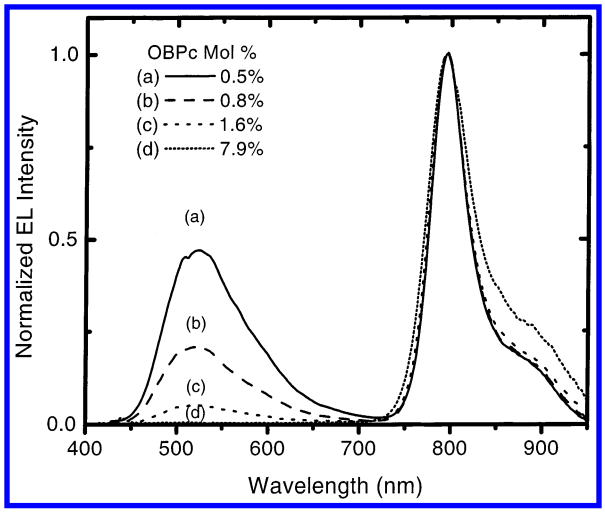

Figure 4. Corrected, normalized (to the guest peak) EL spectra for a series of PVK−Alq_3−OBPc single-layer devices with varying concentration of OBPc (mol % of Alq_3). Host and guest emission is spectrally separated in these Pc- and NPc-doped devices, allowing the relative efficiency of guest emission (with respect to the host) to be measured. Increasing the concentration of the guest has a quenching effect on the host. Most of the device emission is converted to the guest by 0.5 mol %, and between 1.6 and 7.9 mol %, host emission is no longer detected.

single-layer OLEDs.[14] The current/voltage behavior for these devices was essentially unchanged by the addition of the guest dyes, with the exception of slightly increasing turn-on voltages with increasing guest concentration, consistent with other observations of charge trapping.[25] EL spectra were collected for the guest-doped devices at 25 V and were corrected for variations in spectrophotometer efficiency with emission wavelength. The wavelength of maximum emission intensity ($\lambda_{max,EL}$) for all devices is listed in Table 1. In general, the EL spectra are similar to the solution fluorescence spectra in Figure 3. For low guest dye concentrations, EL emission from both the host and guest dyes is easily observed, and their relative intensities are constant with drive voltage after turn-on of the device. Corrected spectra for Alq_3−OBPc−PVK devices are presented in Figure 4 and are typical of the entire series of Pc- or NPc-doped devices, in which the host and guest emission peaks are well separated. The spectra in Figure 4 are normalized to the intensity of the guest emission peak, demonstrating the shift in EL emission to the guest dye with an increase in the guest concentration. For the Pc and NPc devices, host emission fell below detection limits between 1.6 and 7.9 mol % guest concentrations. Devices were compared at guest dye concentrations of 1.6 mol %, at which the host and guest emission could be separately measured and loss of emission due to guest dye self-absorption is minimized, allowing the relative efficiency of guest dye emission (with respect to the host) to be measured.

Comparable devices were also constructed using both DIQA and rubrene as guest dyes, giving EL spectral responses such as those previously reported[6,13−15,23] and comparable to the PL spectra shown in Figure 3. In the case of DIQA and rubrene, the EL response for Alq_3- and $Al(qs)_3$-based devices was completely converted to that of the guest dye at guest concentrations between 1.6 and 7.9 mol %. It is clear that the Pc and NPc guest dyes are comparable in Alq_3 or $Al(qs)_3$ quenching efficiencies during device operation compared to both the quinacridones and rubrene dopants, even though the spectral separation between the host emission and guest absorbance is substantially greater for the Pc and NPc dyes.

Relative Efficiencies of Guest Emission. In these single-layer devices, we assume that electroluminescence leads to guest dye emission primarily by (i) Förster energy-transfer (ET) pathways[26] from the host dye or (ii) by charge-trapping (CT) pathways, in which hole or electron capture by the guest dye is followed by cross-reactions to form the emissive state of the guest dye.[16] We define η_G as the *relative efficiency* of guest dye emission during device operation versus host dye emission, in terms of the separately measured electroluminescence intensities:

$$\eta_G = \frac{I_G/Q_G}{I_H/Q_H + I_G/Q_G} \tag{10}$$

I_G/Q_G and I_H/Q_H are, respectively, the corrected, integrated electroluminescence intensities (peak areas) of both guest dye and host dye (in the presence of each other) in the PVK film normalized to the fluorescence quantum yields (Q_G or Q_H, Table 1) for each species. By including these quantum yield normalizations, η_G can be compared between devices with different host and guest molecules (Table 1). This relative efficiency of guest dye emission during electroluminescence can be written as

$$\eta_G = \eta_{G,ET} + \eta_{G,CT} \tag{11}$$

where $\eta_{G,ET}$ represents the emission of the guest dye due to ET from the host dye and is estimated from host and guest solution spectra (see below) and $\eta_{G,CT}$ represents the emission intensity due to hole or electron capture by the guest dye (CT) followed by $G^{+\bullet}/H^{-\bullet}$ or $PVK^{+\bullet}/G^{-\bullet}$ cross-reactions. $\eta_{G,ET}$ should be the same whether the host is electrically or optically excited, and we assume that other energy-transfer and nonradiative energy-loss pathways not accounted for in the normalizations are the same for all devices, allowing $\eta_{G,CT}$ to be determined from the difference between η_G and $\eta_{G,ET}$ (see below).

In previous quinacridone- and rubrene-doped Alq_3-based OLEDs, a relative measure of ET could be determined by photoexcitation of the host dye in the polymer OLED film at a wavelength that did not overlap the absorbance spectrum of the guest dye. The loss of emission intensity of the host dye could be monitored at a wavelength that did not overlap the emission of the guest dye.[14] Direct determination of ET efficiency for Alq_3 or $Al(qs)_3$ in our Pc- or NPc-doped thin films, however, was not possible because the Soret absorbance bands for these guest dyes significantly overlap the absorbance bands for both Alq_3 and $Al(qs)_3$ hosts. Excitation of Pc or NPc dyes in their Soret band inevitably leads to emission from their lowest excited singlet states.

Values of ET efficiency, $\eta_{G,ET}$, were therefore estimated for each combination of host and guest dyes on the basis of their solution spectroscopic properties and their concentrations in the PVK matrix, assuming that relative values of $\eta_{G,ET}$ determined in solution would extrapolate to this polymer matrix. Values of $\eta_{G,ET}$ were first estimated by comparing values of R_0, the Förster radius, for each dye. R_0 represents the host−guest distance at which ET is 50% efficient and was calculated for each host−guest combination according to[26,30]

$$R_0^{\,6} = \frac{9000\ln(10)\kappa^2 Q_H}{128\pi^5 n^4 N}\int_0^\infty I_H(\lambda)\epsilon_G(\lambda)\lambda^4\,d\lambda \tag{12}$$

κ^2 is a transition dipole orientation factor, which is equal to $^2/_3$ for randomly oriented dipoles with Brownian rotation or 0.476 for randomly oriented, fixed dipoles which is the case in our

TABLE 2: Reaction Energies and Relative Guest Efficiencies for Alq_3/Al(qs)$_3$ Devices

guest dye	$\Delta E°_{PVK^{+\bullet}/G^{+\bullet}}$ (V)[a]	$\Delta E°_{G^{-\bullet}/PVK^{+\bullet}}$ (V)[b]	$\Delta E°_{G^{+\bullet}/H^{-\bullet}}$ (V)[c,d]	$\Delta E°_{H^{-\bullet}/G^{-\bullet}}$ (V)[d,e]	η_G[d,f]	$\eta_{G,ET}$[d,f]	$\eta_{G,CT}$[d,f]
SiPc(THS)$_2$	0.17	2.18	2.84/2.52	0.83/0.51	0.87/0.86	0.81/0.58	0.07/0.28
SiNPc(THS)$_2$	0.55	2.31	2.46/2.14	0.70/0.38	0.85/0.80	0.65/0.45	0.20/0.35
AlOBPcTES	0.66	2.15	2.34/2.03	0.86/0.54	0.90/0.83	0.61/0.39	0.28/0.44
OBPc	0.69	2.14	2.32/2.00	0.86/0.55	0.97/0.93	0.62/0.44	0.35/0.49
OBNPc	0.88	2.11	2.13/1.81	0.90/0.58	0.93/0.90	0.40/0.40	0.52/0.49

[a] $\Delta E°_{PVK^{+\bullet}/G^{+\bullet}} = E°(PVK^{+\bullet}/PVK) - E°(G^{+\bullet}/G)$ (hole capture by guest). [b] $\Delta E°_{G^{-\bullet}/PVK^{+\bullet}} = E°(G/G^{-\bullet}) - E°(PVK^{+\bullet}/PVK)$ (cross-reaction). [c] $\Delta E°_{G^{+\bullet}/H^{-\bullet}} = E°(G^{+\bullet}/G) - E°(H/H^{-\bullet})$ (cross-reaction). [d] First entry for devices made with Alq_3; second entry for devices made with Al(qs)$_3$. [e] $\Delta E°_{H^{-\bullet}/G^{-\bullet}} = E°(G/G^{-\bullet}) - E°(H/H^{-\bullet})$ (electron capture by guest). [f] Standard deviations are approximately 0.01 for all device types.

studies.[36] Q_H is the fluorescence quantum yield of the host, n is the refractive index of the medium, N is Avogadro's number, $I_H(\lambda)$ is the intensity of the corrected emission spectrum of the host (normalized to an area of unity) at wavelength λ, and $\epsilon_G(\lambda)$ is the magnitude of the absorbance spectrum of the guest at wavelength λ in units of molar absorptivity. The validity of this model in describing exciton diffusion and ET in doped organic solids has previously been demonstrated.[37] Because of the poor spectral overlap between Alq_3 emission and absorbance, the rate of ET to the guest is likely to be much higher than the rate of exciton diffusion across Alq_3 molecules.

The values of R_0 are tabulated for each guest dye in Table 1. It is interesting to note that values for the Pc and NPc dyes are comparable to those calculated for both quinacridones and rubrene guest dyes, even though the peak absorbance of these dyes is substantially red-shifted from the peak luminescence of the host. The higher molar absorptivities of these dyes compensates for this, providing for comparable efficiencies of ET. Based on their effective concentrations in the PVK matrix (1.6 mol %), the average distance between guest molecules (R_{G-G}) is 67 Å, the average distance between host molecules (R_{H-H}) is 17 Å, the average distance from a guest molecule to the nearest host molecule (R_{G-H}) is 12 Å, and the average distance from a host molecule to the nearest guest molecule (R_{H-G}) is 22 Å, which is generally smaller than R_0.

Once a value for R_0 is determined, the efficiency of ET, $\eta_{G,ET}$, can be calculated for the case of a solution or film containing randomly distributed host and guest molecules.[26,30,38] It is first necessary to define the critical concentration (C_0), which is the concentration of guest dyes necessary to quench 76% of the host luminescence:

$$C_0 = \frac{3000}{2\pi^{3/2} N R_0^{\,3}} \tag{13}$$

$\eta_{G,ET}$ is then given by

$$\eta_{G,ET} = \sqrt{\pi}\gamma \exp(\gamma^2)[1 - \mathrm{erf}(\gamma)] \tag{14}$$

where $\gamma = C_G/C_0$ and C_G is the effective concentration of the guest.

At this point, values for $\eta_{G,CT}$ estimated from the difference between η_G and $\eta_{G,ET}$ (Table 2) can be correlated with estimates of excess free energies for all possible redox reactions that might occur in the PVK thin film. Solution values of $\Delta E°$ for $PVK^{+\bullet}/G \rightarrow PVK/G^{+\bullet}$ and $H^{-\bullet}/G \rightarrow H/G^{-\bullet}$ charge capture reactions, $G^{+\bullet}/H^{-\bullet}$ and $G^{-\bullet}/PVK^{+\bullet}$ cross-reactions, and relative device, ET, and CT efficiencies for the Alq_3- and Al(qs)$_3$-hosted devices are all considered. $\eta_{G,ET}$ values range from 0.39 to 0.81 and are larger for the Alq_3 devices because the emission peak maximum for Al(qs)$_3$ is blue-shifted ~40 nm from that of Alq_3, decreasing the spectral overlap with the guest dyes. Relative efficiencies for guest dye emission, η_G, are therefore larger for the Alq_3-based devices.

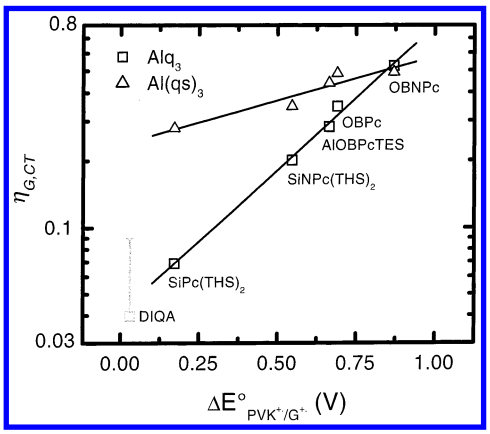

Figure 5. Relative efficiency of guest emission (with respect to the host) due to CT pathways as a function of the reaction energy for hole capture by the guest from $PVK^{+\bullet}$. Devices with Alq_3 (□) and Al(qs)$_3$ (△) as host dyes are presented. The DIQA data point is based on an approximation (see text) and has a large uncertainty in $\eta_{G,CT}$. Uncertainties in $\eta_{G,CT}$ are approximately 0.01 for all other devices.

For devices made from either host dye, $\eta_{G,CT}$ values ranged from 0.07 to 0.52. Plots of $\log(\eta_{G,CT})$ versus the various $\Delta E°$ values in Table 2 were evaluated, but a positive linear correlation was established *only* for $\log(\eta_{G,CT})$ vs $\Delta E°_{PVK^{+\bullet}/G^{+\bullet}}$ (Figure 5). For some of the devices with a large $\Delta E°_{PVK^{+\bullet}/G^{+\bullet}}$ (Alq_3−OBNPc, Al(qs)$_3$−AlOBPcTES, OBPc, OBNPc), $\eta_{G,CT}$ is larger than $\eta_{G,ET}$. As $\Delta E°_{PVK^{+\bullet}/G^{+\bullet}}$ approaches zero, η_G is close to the calculated $\eta_{G,ET}$ for the Alq_3 devices. For Al(qs)$_3$ devices, $\eta_{G,CT}$ approaches 0.25 as $\Delta E°_{PVK^{+\bullet}/G^{+\bullet}}$ approaches zero. Although η_G could not be measured for DIQA and rubrene devices because of their overlapping emission with the host, this value was approximated for Alq_3−DIQA devices by subtracting an assumed host spectrum based on the EL intensity of the host−guest device at 490 nm, at which the guest does not emit. Relative uncertainties in $\eta_{G,CT}$ were substantially higher than those for the Pc and NPc guests because of the approximations involved. Despite this uncertainty, the data suggests that DIQA fits the trend in $\eta_{G,CT}$ (0.04 ± 0.05) vs $\Delta E°_{PVK^{+\bullet}/G^{+\bullet}}$ (0.03 V) defined by the near-IR Pc and NPc guest molecules.

These data suggest that, in these types of thin films, hole capture by the guest dye ($PVK^{+\bullet}/G \rightarrow PVK/G^{+\bullet}$, Figure 6) is the process that controls the rate of excited-state formation in the guest not arising from energy-transfer steps. Once $G^{+\bullet}$ is created, our electrochemical data suggest that this cation radical is stable and the excess free energy in the reaction $G^{+\bullet}/Alq_3^{-\bullet}(Al(qs)_3^{-\bullet} \rightarrow G*/Alq_3(Al(qs)_3$ (as in eq 5) is more than sufficient to produce G*. This is reasonable because the guest dye is present at low concentrations both with respect to PVK and the host dye (Figure 6) and because the excess free energy

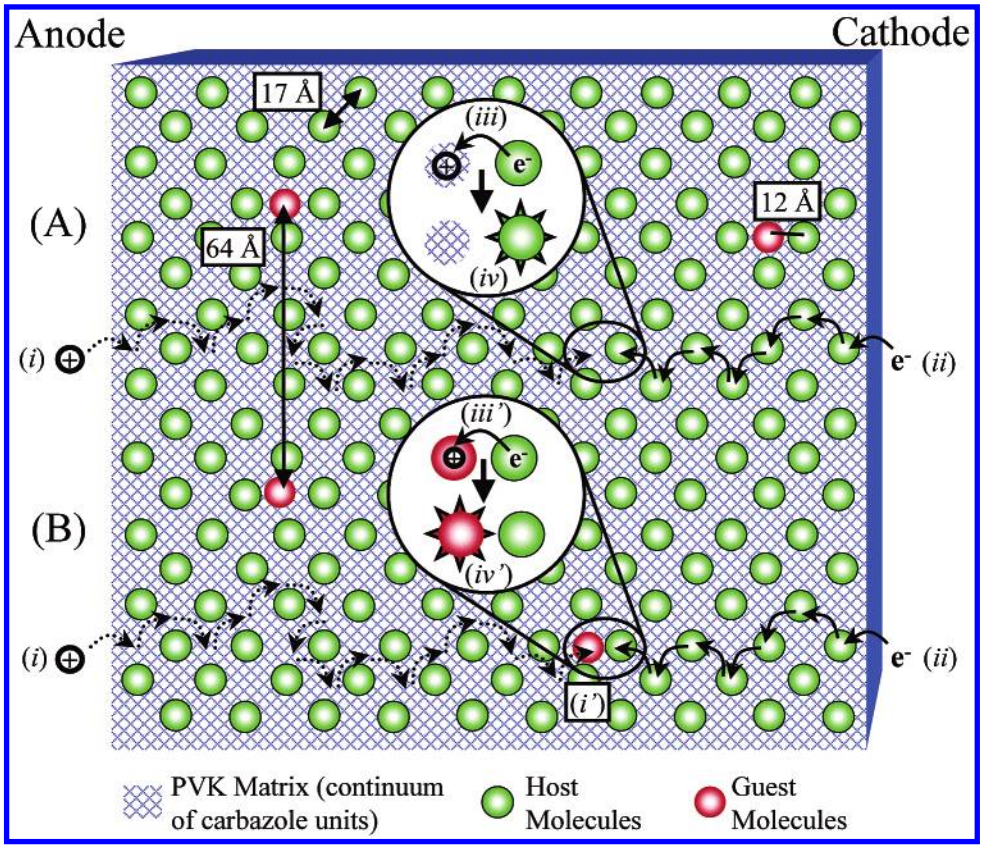

Figure 6. Schematic view of the charge transport, charge-trapping, and recombination steps that lead to host or guest dye emission in PVK-based single-layer OLEDs: (A) in the absence of a guest dye, hole injection and migration in the PVK matrix (i) and electron injection and migration across host dyes Alq_3 or $Al(qs)_3$ (ii) is followed by $PVK^{+\bullet}/Alq_3^{-\bullet}$ recombination reactions (iii, eq 2 in text), leading to Alq_3* emissive states (iv); (B) with guest dyes present, step i can be followed by capture of a hole by the guest dye (i′, eq 6 in text) and $Alq_3^{-\bullet}(Al(qs)_3^{-\bullet})/G^{+\bullet}$ recombination (iii′, eq 7 in text), leading to emissive-state production in the guest dye (iv′). For PVK-based devices with ca. 1.6 mol % of guest dye, the average center to center separation between host dyes is ca. 17 Å, the average separation between guest dyes is ca. 64 Å, and the average separation between a guest dye and the closest host dye is ca. 12 Å. For energy-transfer processes, the critical measurement is the average distance from an excited host molecule to the nearest guest molecule (22 Å, see text).

for the $G^{+\bullet}/Alq_3^{-\bullet}(Al(qs)_3^{-\bullet})$ cross-reactions is between 1.81 and 2.84 eV.

Conclusions

The energetics of hole capture by a guest dye in these doped PVK-based OLEDs appear to control pathways leading to cross-reaction/emissive-state production. Clearly, any OLED guest emissive-state production by ET mechanisms would be preferable if Förster radii for the host/guest combination could be made as large as possible and if charge capture by the guest dye could be avoided entirely. From the electrochemical data shown here and elsewhere,[16−19] however, it is clear that charge capture by guest dyes from hosts such as Alq_3 and various light-emitting polymers is likely and has significant driving forces. For vacuum-deposited two-layer OLEDs based on Alq_3 or comparable lumophores in which the guest dye is doped into the host dye layer, hole capture by the guest dye is less likely. For these devices, it is more likely that electron capture by the guest dye and cross-reactions near the organic/organic′ heterojunction will be the most significant pathway for non-ET emissive-state production. In either event, it is clear that by optimizing CT reactions by guest dyes, light intensities can be increased. Consideration of the excess free energies in the possible cross-reactions occurring in these condensed-phase organic materials may be appropriate for design of optimized device structures and certainly will play a role in extending the emission of these devices to the near-IR. For redox states of host dyes that are unstable, charge capture by the guest dye may also be desirable as a means of enhancing chemical stability of the device.[6,15,27]

Acknowledgment. This research was supported in part by the Office of Naval Research, the National Science Foundation, and the Materials Characterization Program−State of Arizona. The authors are grateful to Jia-Fu Wang and Marie Flore Nabor for the synthesis of the diisoamyl quinacridone (DIQA) and 8-hydroxy-5-piperdinylquinolinesulfonamide ($Al(qs)_3$), respectively.

References and Notes

(1) Greenham, N. C.; Moratti, S. C.; Bradley, D. D. C.; Friend, R. H.; Holmes, A. B. *Nature (London)* **1993**, *365*, 628−630.
(2) Friend, R. H.; Gymer, R. W.; Holmes, A. B.; Burroughes, J. H.; Marks, R. N.; Taliani, C.; Bradley, D. D. C.; Dos Santos, D. A.; Bredas, J. L.; Logdlund, M.; Salaneck, W. R. *Nature* **1999**, *397*, 121−128.
(3) Gustafsson, G.; Cao, Y.; Treacy, G. M.; Klavetter, F.; Colaneri, N.; Heeger, A. J. *Nature (London)* **1992**, *357*, 477−479.
(4) Tang, C. W.; Vanslyke, S. A. *Appl. Phys. Lett.* **1987**, *51*, 913−915.
(5) Tang, C. W.; Vanslyke, S. A.; Chen, C. H. *J. Appl. Phys.* **1989**, *65*, 3610−3616.
(6) Shi, J.; Tang, C. W. *Appl. Phys. Lett.* **1997**, *70*, 1665−1667.
(7) Chen, C. H.; Tang, C. W. *Appl. Phys. Lett.* **2001**, *79*, 3711−3713.
(8) Baldo, M. A.; Thompson, M. E.; Forrest, S. R. *Nature* **2000**, *403*, 750−753.
(9) Adachi, C.; Baldo, M. A.; Thompson, M. E.; Forrest, S. R. *J. Appl. Phys.* **2001**, *90*, 5048−5051.
(10) Lamansky, S.; Djurovich, P.; Murphy, D.; Abdel-Razzaq, F.; Lee, H. E.; Adachi, C.; Burrows, P. E.; Forrest, S. R.; Thompson, M. E. *J. Am. Chem. Soc.* **2001**, *123*, 4304−4312.

(11) Slooff, L. H.; Polman, A.; Cacialli, F.; Friend, R. H.; Hebbink, G. A.; van Veggel, F.; Reinhoudt, D. N. *Appl. Phys. Lett.* **2001**, *78*, 2122−2124.

(12) Cleave, V.; Yahioglu, G.; Le Barny, P.; Friend, R. H.; Tessler, N. *Adv. Mater.* **1999**, *11*, 285−288.

(13) Shaheen, S. E.; Jabbour, G. E.; Kippelen, B.; Peyghambarian, N.; Anderson, J. D.; Marder, S. R.; Armstrong, N. R.; Bellmann, E.; Grubbs, R. H. *Appl.Phys. Lett.* **1999**, *74*, 3212−3214.

(14) Shaheen, S. E.; Kippelen, B.; Peyghambarian, N.; Wang, J. F.; Anderson, J. D.; Mash, E. A.; Lee, P. A.; Armstrong, N. R.; Kawabe, Y. *J. Appl. Phys.* **1999**, *85*, 7939−7945.

(15) Kafafi, Z. H.; Murata, H.; Picciolo, L. C.; Mattoussi, H.; Merritt, C. D.; Iizumi, Y.; Kido, J. *Pure Appl. Chem.* **1999**, *71*, 2085−2094.

(16) Armstrong, N. R.; Wightman, R. M.; Gross, E. M. *Annu. Rev. Phys. Chem.* **2001**, *52*, 391−422.

(17) Armstrong, N. R.; Anderson, J.; Lee, P.; McDonald, E.; Wightman, R. M.; Hall, H. K.; Hopkins, T.; Padias, A.; Thayumanavan, S.; Barlow, S.; Marder, S. *Proc. SPIE−Int. Soc. Opt. Eng.* **1998**, *3476*, 178−187.

(18) Anderson, J. D.; McDonald, E. M.; Lee, P. A.; Anderson, M. L.; Ritchie, E. L.; Hall, H. K.; Hopkins, T.; Mash, E. A.; Wang, J.; Padias, A.; Thayumanavan, S.; Barlow, S.; Marder, S. R.; Jabbour, G. E.; Shaheen, S.; Kippelen, B.; Peyghambarian, N.; Wightman, R. M.; Armstrong, N. R. *J. Am. Chem. Soc.* **1998**, *120*, 9646−9655.

(19) Gross, E. M.; Anderson, J. D.; Slaterbeck, A. F.; Thayumanavan, S.; Barlow, S.; Zhang, Y.; Marder, S. R.; Hall, H. K.; Nabor, M. F.; Wang, J. F.; Mash, E. A.; Armstrong, N. R.; Wightman, R. M. *J. Am. Chem. Soc.* **2000**, *122*, 4972−4979.

(20) Marcus, R. A.; Sutin, N. *Biochim. Biophys. Acta* **1985**, *811*, 265−322.

(21) Marcus, R. A. *J. Electroanal. Chem.* **1997**, *438*, 251−259.

(22) Jang, M.-S.; Song, S.-Y.; Shim, H.-K.; Zyung, T.; Jung, S.-D.; Do, L.-M. *Synth. Met.* **1997**, *91*, 317−319.

(23) Mattoussi, H.; Murata, H.; Merritt, C. D.; Iizumi, Y.; Kido, J.; Kafafi, Z. H. *J. Appl. Phys.* **1999**, *86*, 2642−2650.

(24) (a) Baldo, M. A.; O'Brien, D. F.; Thompson, M. E.; Forrest, S. R. *Phys. Rev. B: Condens. Matter Mater. Phys.* **1999**, *60*, 14422−14428. (b) Ramos-Ortiz, G.; Oki, Y.; Domercq, B.; Kippelen, B. *Phys. Chem. Chem. Phys.* **2002**, *4*, 4109−4114.

(25) (a) Gong, X.; Robinson, M. R.; Ostrowski, J. C.; Moses, D.; Bazan, G. C.; Heeger, A. J. *Adv. Mater. (Weinheim, Ger.)* **2002**, *14*, 581−585. (b) Tessler, N.; Medvedev, V.; Kazes, M.; Kan, S.; Banin, U. *Science* **2002**, *295*, 1506−1508.

(26) Förster, T. *Ann. Phys.* **1948**, *2*, 55.

(27) Aziz, H.; Popovic, Z. D.; Hu, N.-X.; Hor, A.-M.; Xu, G. *Science* **1999**, *283*, 1900−1902.

(28) Wheeler, B. L.; Nagasubramanian, G.; Bard, A. J.; Schechtman, L. A.; Kenney, M. E. *J. Am. Chem. Soc.* **1984**, *106*, 7404−7410.

(29) Sawyer, D. T. Electrochemistry for chemists, 2nd ed.; Wiley: New York, 1995; pp 203−204.

(30) Lakowicz, J. R. *Principles of fluorescence spectroscopy*; Plenum Press: New York, 1983.

(31) Hopkins, T. A.; Meerholz, K.; Shaheen, S.; Anderson, M. L.; Schmidt, A.; Kippelen, B.; Padias, A. B.; Hall, H. K., Jr.; Peyghambarian, N.; Armstrong, N. R. *Chem. Mater.* **1996**, *8*, 344−351.

(32) Mezza, T.; Armstrong, N. R.; Kenney, M. *J. Electroanal. Chem. Interfacial Electrochem.*; **1984**, *176*, 259−273.

(33) Ford, W. E.; Rodgers, M. A. J.; Schechtman, L. A.; Sounik, J. R.; Rihter, B. D.; Kenney, M. E. *Inorg. Chem.* **1992**, *31*, 3371−3377.

(34) Aoudia, M.; Cheng, G.; Kennedy, V. O.; Kenney, M. E.; Rodgers, M. A. J. *J. Am. Chem. Soc.* **1997**, *119*, 6029−6039.

(35) Shoustikov, A.; You, Y.; Burrows, P. E.; Thompson, M. E.; Forrest, S. R. *Synth. Met.* **1997**, *91*, 217−221.

(36) Steinberg, I. Z. *Annu. Rev. Biochem.* **1971**, *40*, 83−114.

(37) Ferguson, J. *Aust. J. Chem.* **1956**, *9*, 172−179.

(38) Förster, T. *Discussions Faraday Soc.* **1959**, *No. 27*, 7−17.